Electric Power Systems Research 259 (2026) 113201

Contents lists available at ScienceDirect

Electric Power Systems Research

journal homepage: www.elsevier.com/locate/epsr

Cost-effective power system expansion planning under uncertainty considering fast EV charging stations with integrated energy storage support

Yuxin Sun [a], Stefan Borozan [a], Tala El Samad [b,*], Guibin Wang [c], Goran Strbac [a]

[a] Department of Electrical and Electronic Engineering, Imperial College London, London, SW7 2AZ, United Kingdom
[c] Department of Engineering, City St George's, University of London, London, EC1V 0HB, United Kingdom
[c] College of Mechatronics and Control Engineering, Shenzhen University, Shenzhen, 518060, China

A R T I C L E I N F O

Keywords:
Fast EV charging stations
Energy storage system
Electric vehicles
Network expansion planning
Option value
Benders decomposition

A B S T R A C T

The electrification of transport through electric vehicles is accelerating urban sustainability. Fast charging stations (FCS) are vital to this transition due to their high power and short turnaround times. However, scaling up electrified transport requires substantial investment in high-capacity charging infrastructure and power network reinforcement to meet charging demand. The long-term impact of FCS development on network expansion planning remains underexplored, especially under uncertainty. This paper proposes two FCS models: standalone and integrated with energy storage (ESS-FCS), to explore their strategic and economic value as non-wire investment options under uncertainty. A 40-year multi-stage stochastic planning framework is developed, leveraging scenario trees and Benders decomposition which ensure scalability and decision flexibility. Real option valuation is applied to quantify the investment value of ESS-FCS, highlighting its role in mitigating overinvestment and stranded asset risks. Case studies on modified Garver 6-bus (transmission) and IEEE 33-bus (distribution) systems reveal potential economic benefits of up to £292.06 million. Sensitivity analysis on charger ratings further demonstrates the adaptability and strategic advantage of ESS-FCS in evolving low-carbon power system landscapes.

1. Introduction

1.1. Motivation

Mounting evidence of global warming, driven by greenhouse gas emissions, has placed climate change firmly at the center of global policy [1]. This is reflected in initiatives such as the Paris Agreement [2] and the UK's Net Zero Strategy [3]. Concurrently, rising fuel prices and environmental concerns have accelerated the shift from internal combustion engine vehicles to electrified transport [4]. Electric vehicles (EVs) have become widely recognized as a zero-emission alternative. Governments are actively promoting EV adoption and expanding charging infrastructure, particularly fast charging stations (FCSs) because of their high efficiency and rapid charging capabilities [5–7]. With the increase in EV uptake, electricity demand is expected to rise significantly. High-power FCS loads are both variable and demanding, which creates challenges for network planning. Substantial investments are required to avoid demand curtailment and maintain grid instability. Moreover, long-term power system development is complicated by uncertainties in EV adoption rates, policy changes, technology costs, and renewable integration. These uncertainties raise the risk of premature or misaligned investments. To address these challenges, a planning framework that incorporates FCSs and accounts for uncertainty is essential. Integrating energy storage systems (ESS) with FCSs offers operational flexibility by decoupling charging cycles from grid imports. However, the strategic role of ESS-FCS in network expansion and investment decision-making, particularly with regards to their potential in mitigating long-term uncertainty, is still insufficiently explored.

1.2. Literature review

Optimizing the planning of FCS has become a key research area as EV adoption grows. For example, Ref. [5] studies FCS allocation in an integrated electricity-gas system, focusing on carbon emissions while satisfying EV charging demands. Ref. [8] introduces an adaptive FCS

* Corresponding author at: Tala El Samad City St George's University of London, United Kingdom of Great Britain And Northern Ireland, United Kingdom.
E-mail address: t.elsamad@citystgeorges.ac.uk (T.E. Samad).

https://doi.org/10.1016/j.epsr.2026.113201
Received 22 September 2025; Received in revised form 30 March 2026; Accepted 23 April 2026
Available online 9 May 2026

Nomenclature

A. Sets and indices

Ω_G	Set of all generation units, indexed g
Ω_L	Set of all transmission or distribution lines, indexed l
Ω_M	Set of all scenario tree nodes, indexed m
$\Omega_{M(s)}$	Set of all nodes belonging to scenario s
Ω_S	Set of all scenarios, indexed s
Ω_N	Set of all network buses, indexed n
Ω_T	Set of time periods, indexed t
$\mathscr{P}^{ESS}_{(m)}$	Set of ancestor nodes of node m within the lifetime of ESS
$\epsilon(m)$	Scenario tree stage to which node m belongs

B. Decision variables

α^i_m	Auxiliary variable at i th iteration at scenario tree node m
$\iota_{m,l}$	Size of transmission capacity invested
$\widetilde{\iota}_{m,l}$	Aggregate transmission capacity invested that is operational at node m
$\sigma^{L,i}_{m,l}$	Dual variable related to transmission capacity investments
$\sigma^{ESS/FCS,i}_{m,n}$	Dual variable related to ESS or FCS investments
$d_{m,n,t}$	Curtailed non-public EV demand
$d^{public}_{m,n,t}$	Curtailed public EV demand
$P^{gen}_{g,m,t}$	Generator output power
$P^{+}_{m,n,t}$	Charging power of ESS from grid
$P^{CH}_{m,n,t}$	Charging power of FCS via ESS (Discharging)
$S^{ESS}_{m,n}$	Size of ESS capacity invested
$\widetilde{S}^{ESS}_{m,n}$	Aggregate ESS capacity invested that is operational at node m
$SOC_{m,n,t}$	State of charge of ESS
$X^{FC}_{m,n}$	Number of FC units invested
$\widetilde{X}^{FC}_{m,n}$	Aggregate number of FC units invested that are operational at node m
$X_{m,l}$	Binary variable deciding line investments

C. Input parameters

$\eta^{\pm}_{ESS}$	Charging/Discharging efficiencies of ESS
$\iota^{min/max}_l$	Minimum/Maximum investment capacity of line l
$\lambda_{n,t}$	Load factor for non-public EV demand
$\lambda^{pubilc}_{n,t}$	Load factor for public EV demand
τ	Duration of time period t in hour
$\theta_{m,x/y,t}$	Load angle
π_m	Probability of scenario tree node m
b_l	Susceptance
$c^{L,f}_l$	Fixed line investment costs in £ of l
$c^{L,v}_l$	Variable line investment costs in £ of l
c^{ESS}_m	ESS investment costs in £ in m
c^{FC}_m	Individual fast charger investment costs in £ in m
$D_{m,n,t}$	Peak non-public EV demand at bus n, scenario tree node m, time period t
$D^{public}_{m,n,t}$	Peak public EV demand at bus n, scenario tree node m, time period t
$G_{g,n}$	Generator-to-line incidence matrix
$I_{l,n}$	Bus-to-line incidence matrix
L_l	Length of line l
$N^{public}_{m,n}$	Public EV number at bus n
P^{FC}	Individual fast charger rating
$P^{max}_{g,m,t}$	Maximum output power of generator
$R^{ESS/FC/L}_{\epsilon(m)}$	Cumulative discount factor for ESS/fast charger /line investment costs in stage to which m belongs
$R^{O}_{\epsilon(m)}$	Cumulative discount factor for operational costs in stage to which m belongs
$R^{down/up}_g$	Ramp down/up capability of generators
$s^{min/max}$	Minimum/Maximum ESS capacity investment
$SOC^{min/max}$	Minimum/Maximum state of charge of ESS
V^{CH}	FCS-ESS operational cost in £
V^{VOLL}	Demand curtailment cost in £
V^{gen}_g	Generation operational cost in £ of generator g
$Y_{m,l,t}$	Power flow

strategy within a multi-stage expansion planning. Ref. [9] presents a bilevel mixed-integer FCS planning model to minimize traffic time and investment costs, incorporating EV charging behavior and self-service routing. A case study in [10] uses real-road network data and a genetic algorithm to demonstrate optimal FCS planning for Al Ain City.

Incorporating ESS into FCS infrastructure has become a crucial strategy to smooth energy demand profiles [7], mitigate charging load fluctuations [11,12], and offset renewable energy generation variability [7,13]. To determine optimal ESS sizing in planned FCS, [7] focuses on minimizing costs, improving EV resilience, and reducing peak loads. The study finds that punitive peak-hour electricity prices have a stronger influence on ESS scale than general market price increases. Ref. [13] examines the optimal FCS design that integrates wind, PV, and ESS. It proposes a multi-objective optimization algorithm to minimize electricity costs and emissions. The results show that integrated ESS can reduce the adverse effects of wind power uncertainty. Ref. [14] applies a mixed-integer linear programming (MILP) framework for electric-bus charging stations. The study determines optimal FCS and ESS sizing and highlights the great potential of ESS in reducing charging costs. Ref. [15] investigates joint planning of FCS with PV and ESS to reduce carbon emissions and satisfy the demand of delivery fleets, confirming environmental benefits. Ref. [16] proposes adjusting fixed ESS scale in FCS based on the average acceptable driver wait times. In [17], stochastic programming is used to design optimal FCS capacity. Findings reveal that ESS integration can reduce line reinforcement needs by 35 % and mitigate wind power variability.

Since storage-integrated FCSs can provide significant flexibility to support power system operation, most existing studies focus on operational benefits or charging infrastructure deployment problems. Their potential role as a flexible investment option within long-term network expansion planning under uncertainty, and the associated economic value, remain largely underexplored. Most existing studies rely on static investment evaluation methods, like Net Present Value (NPV) [15, 18–21], which simplify investment decisions into rigid “now or never” choices based on discounted future revenues and costs. These approaches exhibit inherent limitations in capturing the complexity of long-term infrastructure investments under uncertainty, as they overlook the value of timing flexibility and the opportunity cost of premature investment. Real Option (RO) theory offers a more advanced framework for evaluating investment flexibility under uncertainty [22–29]. It considers an investment worthwhile not only when revenues exceed costs but also offset the opportunity cost of exercising the investment option prematurely. RO accounts for the value of delaying action to await better information or market conditions. This is especially relevant for FCS infrastructure, where investors face uncertainty in EV adoption, electricity prices, and regulatory changes. ESS-FCS projects, being capital-intensive and difficult to reverse, are particularly sensitive to timing flexibility, making RO a suitable tool for assessing their strategic value.

Recognizing these challenges, recent studies have explored RO applications in smart grid planning [22], renewable energy development [23], demand-side management and storage [24], and smart charging [25,26]. Ref. [27] applies RO to rooftop PV projects, showing that many would be prematurely rejected under NPV analysis alone, highlighting the superiority of RO. As power systems grow more complex, traditional RO valuation techniques, such as Black-Scholes partial differential equation models [30], lattice models [4,25,26,28] or simulation models [29,31], increasingly need to be combined with planning frameworks to better simulate uncertainties and their impacts. This paper applies the scenario tree method, implemented within a multi-stage stochastic optimization planning framework to comprehensively capture investment flexibility under uncertainty and the economic potential of the investment options, quantified as option value (OV).

1.3. Contributions

This research examines the strategic role and economic value of FCSs integrated with ESS as a non-wire solution for expansion planning under uncertainty. The contribution is primarily methodological, focusing on the development of a generalizable multi-stage stochastic planning and valuation framework. The case studies are designed accordingly to demonstrate the applicability and robustness of the proposed approach. The key contributions include:

i. A multi-stage stochastic network expansion planning framework is formulated for both distribution and transmission networks, aiming to minimize expected system costs. Scenario trees model long-term uncertainty, enabling flexible decision making, such as delaying, expanding, or modifying investments as conditions evolve, to avoid premature investments and stranded asset risks, while enhancing economic efficiency by adapting to a range of potential future scenarios. For computational tractability, a multi-cut Benders decomposition algorithm is applied to solve the mixed-integer combinatorial problem.

ii. A novel ESS-FCS investment and operational model is developed and integrated within the planning framework to evaluate its strategic and economic value. A comparative FCS-only model is also developed to assess the added benefit of ESS in improving FCS performance and flexibility.

iii. A real options-based economic assessment is implemented to quantify the value of investment flexibility offered by ESS-FCS under uncertainty. The analysis highlights its role in mitigating overinvestment and reducing stranded asset risks in network development.

iv. The framework is applied to modified IEEE 33-bus and Garver 6-bus systems. Sensitivity analysis on fast charger (FC) ratings illustrates planning complexities and demonstrates the superior strategic value of ESS-FCS across diverse scenarios.

1.4. Organization of this paper

The remainder of this paper is structured as follows. Section 2 presents the proposed models for FCS, both with and without ESS integration. Section 3 details the long-term stochastic expansion planning framework with integrated FCS models. Section 4 features case studies demonstrating the strategic significance of ESS-FCS in active distribution networks, and its economic value in transmission networks. Finally, Section 5 concludes with a summary of the main findings.

2. Fast EV charging station models

The FCS models evaluated in this paper are illustrated in Fig. 1. The first is a standalone FCS without ESS, referred to as the FCS-only model. The second integrates energy storage, referred to as the ESS-FCS model. In the FCS-only model (Fig. 1(a)), the station is directly connected to the grid via rectifiers and essential equipment. Power drawn from the grid depends on the EV charging demand profile, which can lead to significant demand peaks and potential network congestion, especially in distribution systems. The ESS-FCS model (Fig. 1(b)) addresses these issues by allowing the station to operate independently of real-time charging demand. It draws power from the grid during low-demand or low-price periods and supplies stored energy during peak times. This reduces charging costs and alleviates grid stress. Directional arrows indicate power flow: the grid supplies energy to the charging station, while the ESS and FCS are interlinked via a rectifier. The ESS stores surplus energy and discharges it as needed, improving network utilization and influencing investment decisions.

3. Long-term stochastic network expansion planning framework

3.1. Overview of the proposed planning framework

Fig. 2 illustrates the proposed multi-stage stochastic network expansion planning framework integrated with FCS models. This framework enables adaptive and informed investment decisions under uncertainty, considering both conventional reinforcement and smart grid technologies such as FCS and ESS. It takes EV charging profiles, generation and demand data, and network topology as inputs, while effectively incorporating uncertainties into the planning process. Uncertainties in power system and charging infrastructure planning may arise from technical, economic, and regulatory factors such as load growth, EV adoption, renewable capacity and location, electricity price volatility, technology costs, and policy changes. Accurately modelling these uncertainties is essential for robust long-term planning. This study

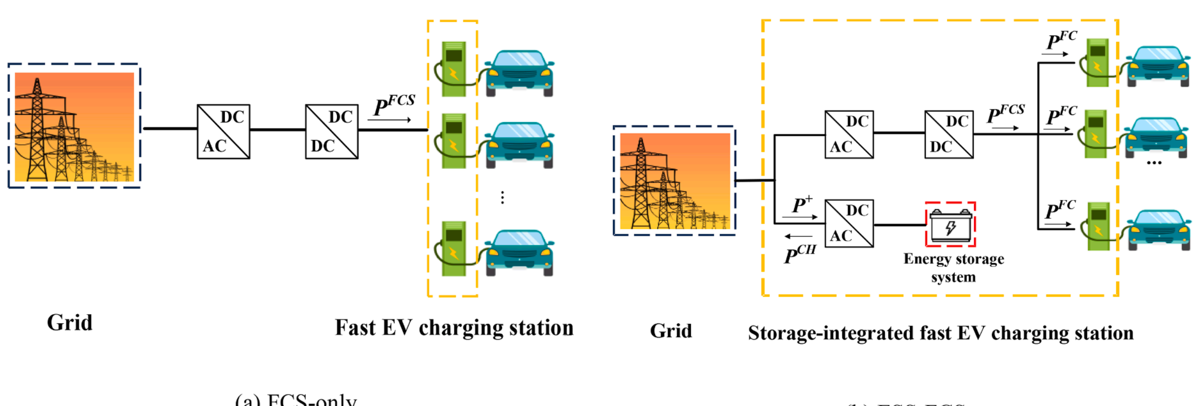

Fig. 1. The illustrative diagrams of two fast EV charging station models.

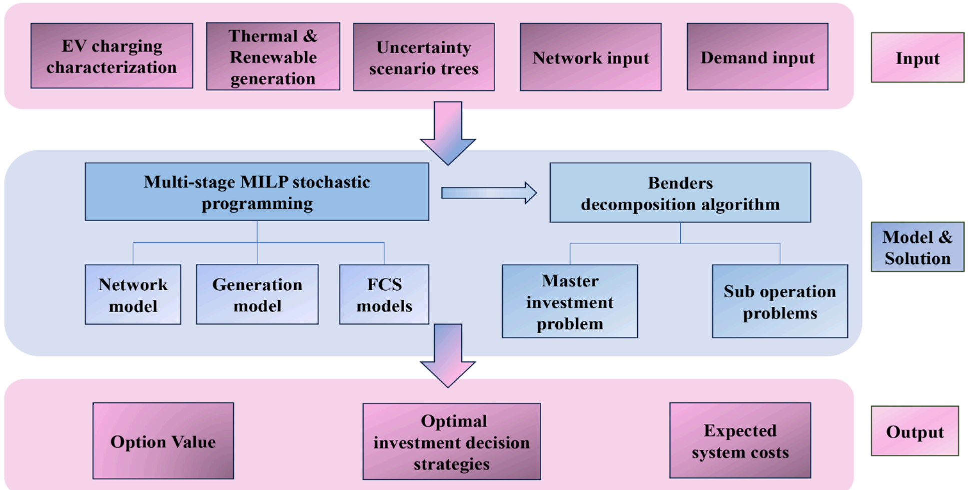

Fig. 2. The proposed multi-stage stochastic expansion network planning framework.

focuses on uncertainties related to FC unit investment costs, installed renewable capacity, and public EV fleet size, as these directly affect infrastructure demand, system flexibility, and the performance of investment options. While these are the focus here, other relevant uncertainties can be incorporated similarly.

The framework employs scenario trees to capture possible future developments and their interdependencies, enabling a systematic evaluation of investment decisions under uncertainty. By solving a multi-stage stochastic optimization problem, it produces optimal investment strategies, discounted expected system costs, and the associated OV, defined here as the total expected system savings achieved when planning with the ESS-FCS option rather than the FCS-only baseline. While classical RO theory interprets OV as the premium arising from investment flexibility, both cases in this research are evaluated within a modelling framework that already embeds timing flexibility. Consequently, the reported OV reflects the incremental value of the ESS-FCS investment option relative to the business-as-usual alternative, ensuring conceptual consistency while focusing on the comparative value of alternative real investment options.

3.2. Mathematical formulation

The objective of the proposed planning framework is to determine an optimal long-term network expansion strategy under multi-dimensional uncertainties across scenario nodes. This involves evaluating multiple investment possibilities considering type, scale, location, and timing. Due to the complexity and stochastic nature of the problem, a large number of decision variables are involved. The deterministic equivalent of this large-scale problem is formulated as a MILP, as defined by Eqs. (1)-(25).

$$\min_{\mathbf{x}_m}\left\{\sum_{\forall m}\pi_m\left[V_m^I(\mathbf{x}_m)+V_m^O(\mathbf{x}_m)\right]\right\} \tag{1}$$

where

$$\begin{aligned} V_m^I = R^L_{\varepsilon(m)}\sum_{\forall l\in\Omega_L}\left(c_l^{L,f}X_{m,l}+c_l^{L,v}\iota_{m,l}\right)L_l+ \\ R^{FC}_{\varepsilon(m)}\sum_{\forall n\in\Omega_N}c_m^{FC}X_{m,n}^{FC}+R^{ESS}_{\varepsilon(m)}\sum_{\forall n\in\Omega_N}c_m^{ESS}S_{m,n}^{ESS} \end{aligned} \tag{2}$$

$$V_m^O=R^O_{\epsilon(m)}\sum_{\forall t\in\Omega_T}\tau\left[\sum_{\forall g\in\Omega_G}V_g^{gen}P_{g,m,t}^{gen}+\sum_{\forall n\in\Omega_N}V^{CH}P_{m,n,t}^{CH}+\sum_{\forall n\in\Omega_N}V^{VOLL}\left(d_{m,n,t}+d_{m,n,t}^{public}\right)\right] \tag{3}$$

subject to

$$X_{m,l}\in\{0,1\},\forall m,l \tag{4}$$

$$\sum_{m\in\Omega_{M(s)}}X_{m,l}\le 1,\forall s,l \tag{5}$$

$$\iota_{m,l}\ge 0 \tag{6}$$

$$X_{m,l}\iota_l^{min}\le\iota_{m,l}\le X_{m,l}\iota_l^{max},\forall m,l \tag{7}$$

$$\tilde{\iota}_{m,l}=\sum_{a\in\{1,\dots,\varepsilon(m)-1\}}\iota_{a,l},\forall m,l \tag{8}$$

$$X_{m,n}^{FC}\in\mathbb{Z}^+,\forall m,n \tag{9}$$

$$\sum_{a\in\{1,\dots,\varepsilon(m)\}}X_{a,n}^{FC}\le N_{m,n}^{public},\forall m,n \tag{10}$$

$$\tilde{X}_{m,n}^{FC}=\sum_{a\in\{1,\dots,\varepsilon(m)\}}X_{a,n}^{FC},\forall m,n \tag{11}$$

$$S_{m,n}^{ESS}\ge 0 \tag{12}$$

$$s^{min}\le S_{m,n}^{ESS}\le s^{max},\forall m,n \tag{13}$$

$$\tilde{S}_{m,n}^{ESS}=\sum_{\alpha\in\mathscr{P}_{(m)}^{ESS}}S_{\alpha,n}^{ESS},\ \forall m,n \tag{14}$$

$$SOC_{m,n,T_m}=SOC_{m,n,0},\forall m,n \tag{15}$$

$$SOC_{m,n,1}=SOC_{m,n,0}+\tau\left(\eta_{ESS}^+P_{m,n,1}^+-\frac{P_{m,n,1}^{CH}}{\eta_{ESS}^-}\right),\forall m,n \tag{16}$$

$$SOC_{m,n,t}=SOC_{m,n,t-1}+\tau\left(\eta_{ESS}^+P_{m,n,t}^+-\frac{P_{m,n,t}^{CH}}{\eta_{ESS}^-}\right),\forall m,n,t\backslash\{t_1\} \tag{17}$$

$$SOC^{min}\le SOC_{m,n,t}\le SOC^{max},\forall m,n,t \tag{18}$$

$$0\le P_{m,n,t}^+\le C_{max}^{ESS}\tilde{S}_{m,n}^{ESS},\forall m,n,t \tag{19}$$

$$D_{m,n,t}^{public}\lambda_{n,t}^{public}-d_{m,n,t}^{public}\le P_{m,n,t}^{CH}\le P^{FC}\tilde{X}_{m,n}^{FC},\forall m,n,t \tag{20}$$

$$0 \leq P_{g,m,t}^{gen} \leq P_{g,m,t}^{max}, \forall g, m, t \quad (21)$$

$$P_{g,m,t-1}^{gen} - \tau R_{g}^{down} \leq P_{g,m,t}^{gen} \leq P_{g,m,t-1}^{gen} + \tau R_{g}^{up}, \quad \forall g \in \Omega_G, m, t \in \{\Omega_T - 1\} \quad (22)$$

$$Y_{m,l,t} = b_l\left(\theta_{m,x_1,t} - \theta_{m,y_1,t}\right), \forall m, l, t \quad (23)$$

$$\left|Y_{m,l,t}\right| \leq \iota_{m,l}^{0} + \widetilde{\iota}_{m,l}, \forall m, l, t \quad (24)$$

$$\sum_{\forall g \in \Omega_G} G_{g,n} P_{g,m,t}^{gen} + \sum_{\forall l \in \Omega_L} I_{l,n} Y_{m,l,t} = P_{m,n,t}^{+} + D_{m,n,t}\lambda_{n,t} - d_{m,n,t}, \forall m, n, t \quad (25)$$

Eqs. (1)-(3) define the objective function, which minimizes the expected total system cost, comprising investment costs (V_m^I) and operational costs (V_m^O). Investment costs, as defined in Eq. (2), include conventional line reinforcements, FCS, and ESS components. Operational costs, presented in Eq. (3), cover generation, FCS operation, and load curtailment. Cumulative discount factors ($R_{\varepsilon(m)}$) are influenced by the prevailing interest rates relevant to various components and different stages. For clarity, dependencies on decision variables within these equations are not explicitly shown.

Then, Eqs. (4)-(14) constrain investment decisions: Eqs. (4)-(8)-(8) focus on the transmission network assets, where Eq. (4) defines the binary decision variable corresponding to line investment decisions, Eq. (5) ensures that single investment per asset and scenario, Eq. (6) defines the continuous nature of capacity upgrade decisions, Eq. (7) sets the capacity limits, and Eq. (8) informs the amount of invested capacity in each line l that is operational in scenario tree node m, accounting for construction delays of one scenario tree stage. Eqs. (9)-(11) focus on FCS investments where Eq. (9) specifies the non-negative integer nature of FCs investment decision variables, Eq. (10) imposes limits based on public EV fleet size, Eq. (11) informs the total number of installed FCs in each scenario tree node, assuming that investments are not subject to a notable construction delay. ESS investments are governed by Eqs. (12)-(14), where Eq. (12) defines the continuous decision variable for ESS capacity investment, Eq. (13) imposes the limits on this capacity, and Eq. (14) aggregates ESS capacities that have been invested and remain within the assumed technical lifetime of storage and thereby contribute to the available operational capacity at node m. Similar to FCS, ESS capacity is available in the same stage that the investment decision takes place. This stage-zero deployment approximation may slightly overestimate operational benefits in the initial stage; however, it does not materially affect long-term outcomes.

System operation is modelled with Eqs. (15)-(25). Eq. (15) initializes the state of charge (SOC) of ESS units and mandates that SOC should be the same at the beginning and the end of the time period covered by Ω_T. Eq. (16) and (17) update the SOC for all units in the first and each successive time interval, where t_1 represents the first period in time period Ω_T. Eq. (18) specifies the permissible operational range for the SOC. ESS charging power is constrained by the available capacity in Eq. (19), where C_{max}^{ESS} is the C-rate of the ESS, representing the intrinsic capability of the ESS to charge or discharge relative to its rated energy capacity. $P_{m,n,t}^{CH}$ is constrained in Eq. (20) where the upper limit is the total charging power of installed FCs and the lower limit is the demand for public EV fast charging accounting for curtailment. Power generation is constrained with Eq. (21) and generator ramping is modelled with Eq. (22). The DC power flow approximation is employed with Eq. (23) and (24), where the latter constrains power flows to the available line capacities in the current scenario tree node m. Finally, Eq. (25) establishes the power balance, ensuring that net power injection at each bus equal zero across all time period. Note that the balance constraint implies that, with the ESS-FCS concept, EV fast charging demand is decoupled from power delivery from the grid.

3.3. Solution method

A key challenge in the multi-stage stochastic planning model is its scale. As the number of scenarios and stages increases, so does the number of decision variables and constraints. Therefore, the hierarchical multi-cut Benders decomposition method, used in [25,28], is employed in this work, as outlined in Table 1.

The original multi-stage stochastic problem is decomposed into a master problem and a set of sub-problems by relaxing complicating constraints. Although expressed differently, this decomposition primarily draws from the objective functions and constraints detailed in the previous subsection. The master problem is centered around investment. By integrating the investment objective function (Eq. (2)), auxiliary variables (α_m^i) are introduced to approximate the sub-problem's objective function within the original one. Consequently, the revised objective function of the master problem is structured as Eq. (26).

$$min R_{\varepsilon(m)}^{L} \sum_{\forall l \in \Omega_L} \left(c_l^{L,f} X_{m,l} + c_l^{L,v} \iota_{m,l}\right) L_l + R_{\varepsilon(m)}^{FC} \sum_{\forall n \in \Omega_N} c_m^{FC} X_{m,n}^{FC} + R_{\varepsilon(m)}^{ESS} \sum_{\forall n \in \Omega_N} c_m^{ESS} S_{m,n}^{ESS} X^{ESS} + \alpha_m^i \quad (26)$$

The master problem encompasses constraints outlined in Eqs. (4)-(14), each pertaining to investment decisions. Additional constraints are introduced based on duality theory, as shown in Eq. (27).

$$\alpha_m \geq V_m^{O(i-1)} + \sum_{\forall l} \sigma_{m,l}^{L,i}\left(y_{m,l}^{L} - y_{m,l}^{L,i-1}\right) + \sum_{\forall n} \sigma_{m,n}^{FCS,i}\left(y_{m,n}^{FCS} - y_{m,l}^{FCS,i-1}\right) + \sum_{\forall n} \sigma_{m,n}^{ESS,i}\left(y_{m,n}^{ESS} - y_{m,l}^{ESS,i-1}\right) \quad (27)$$

The sub-problems handle system operation using the objective in Eq. (3) and constraints (15)-(25). The master and sub-problems are linked using complicating constraints and Lagrange multipliers Eqs. (28)-(30).

$$\iota_{m,l} = y_{m,l}^{L,i} : \sigma_{m,l}^{L,i} \quad (28)$$

$$N_{m,n}^{FC} = y_{m,n}^{FCS,i} : \sigma_{m,l}^{FCS,i} \quad (29)$$

$$S_{m,n}^{ESS} = y_{m,n}^{ESS,i} : \sigma_{m,n}^{ESS,i} \quad (30)$$

This algorithm proceeds iteratively. In each iteration, i, the master problem determines investment decisions. These are passed to the sub-problems, which compute operational costs and dual variables. Benders cuts are then appended to the master problem in the ensuing iteration to improve the operation costs approximation, leading to more accurate investment decisions. This process continues until convergence is achieved.

Table 1
Benders decomposition solution method.

Step 0	**Initialization** Set Benders iteration index $i = 1$. Obtain all necessary input data for the problem. Set the initial lower bound as $Z_l^0 = 0$ and the initial upper bound as $Z_u^0 = +\infty$.
Step 1	**Master problem solution** Solve master problem to obtain investment decisions and expected investment costs. Update upper bound $Z_u^i = \sum_{m \in \Omega_M} V_m^{I(i)}$.
Step 2	**Sub-problem solution** Solve all sub-problems with investment decisions, get expected operation costs and all dual variable values. Update lower bound $Z_l^i = V_m^{O(i)}$.
Step 3	**Convergence check** If $\frac{Z_u^i - Z_l^i}{Z_u^i} \leq \zeta$ where ζ is a predefined value close to 0, then the optimal solution is obtained, otherwise append the Benders optimality cuts to the master problem, set $i = i + 1$, and go to **Step 1**.

4. Case studies

This section presents case studies to evaluate the proposed ESS–FCS planning framework under uncertainty. The modified IEEE 33-bus distribution system is used to analyze the impact of ESS–FCS on investment timing and network reinforcement decisions, including sensitivity analyses on renewable penetration and scenario probabilities. The modified Garver 6-bus transmission system is then considered to quantify the economic value of ESS–FCS for different fast-charger ratings. Computational results are lastly reported to demonstrate the tractability of the proposed solution approach.

4.1. Strategic role of ESS-FCS in active distribution networks

A modified IEEE 33-bus system [32] is used to assess the strategic role of ESS-FCS in active distribution networks. The system includes 33 buses, 32 fixed lines, 5 switchable lines, and 5 generators (thermal and PV). PV units are located at buses 18, 22, 25, and 33, while bus 1 serves as the grid supply point. Buses 9–33 are designated residential EV areas, and others may host public EV charging hubs. To simulate a medium-voltage network, non-EV demand in [32] is scaled by a factor of 10.

Uncertainties in EV adoption, FC unit investment cost [33], and renewable capacity are modelled using the scenario tree in Fig. 3, spanning four planning stages: 2020, 2030, 2040, and 2050. It includes 6 scenarios and 13 nodes, capturing variations in public EV presence (PEV[.]), EV counts (PEV{.}), FC unit investment costs (C{.}), and PV generator capacities, in MW, at bus 18, 22, 25 and 33, respectively (S{a, b,c,d}).

A 5 % growth per-decade in non-EV load, with load factors based on [33,34], ensures EV demand remains within 40 % of baseline demand. The scenario tree shows the transition and scenario probabilities, while not based on empirical data the probabilities are chosen to illustrate plausible dynamics within the planning context. The lifetime of ESS is set to 15 years [34]. ESS aging is modeled using this fixed lifetime assumption, which is consistent with long-term expansion planning practice. High-resolution cycle-dependent degradation dynamics are not incorporated, as the present study focuses on strategic multi-stage investment decisions. Note that these assumptions mainly improve the computational performance of the multi-stage planning problem and may slightly affect the exact timing of investments, but they do not materially alter the main conclusions regarding the strategic and economic value of ESS-FCS.

Three investment options are considered: line reinforcement, FC installation, and ESS capacity. The associated costs for investment options are based on [33–37] are listed Table 2. Note that distribution lines can be upgraded only once, and the cost of a thermal generator accounts for both electricity generation and CO_2 emission costs. The assumed rating of a single FC is 50 kW.

The results for optimal line investments across scenarios are shown in Fig. 4, with [x–y] denoting upgraded lines and {z} indicating

Table 2
Unit investment costs of IEEE 33-bus system [33–37].

Investment option	Cost
Fixed line reinforcement (£/km)	35,000
Variable line reinforcement (£/MW)	35
ESS in stage 1 (£/EV)	16,000
ESS in stage 2 (£/EV)	14,000
ESS in stage 3 (£/EV)	11,000
ESS in stage 4 (£/EV)	9,000

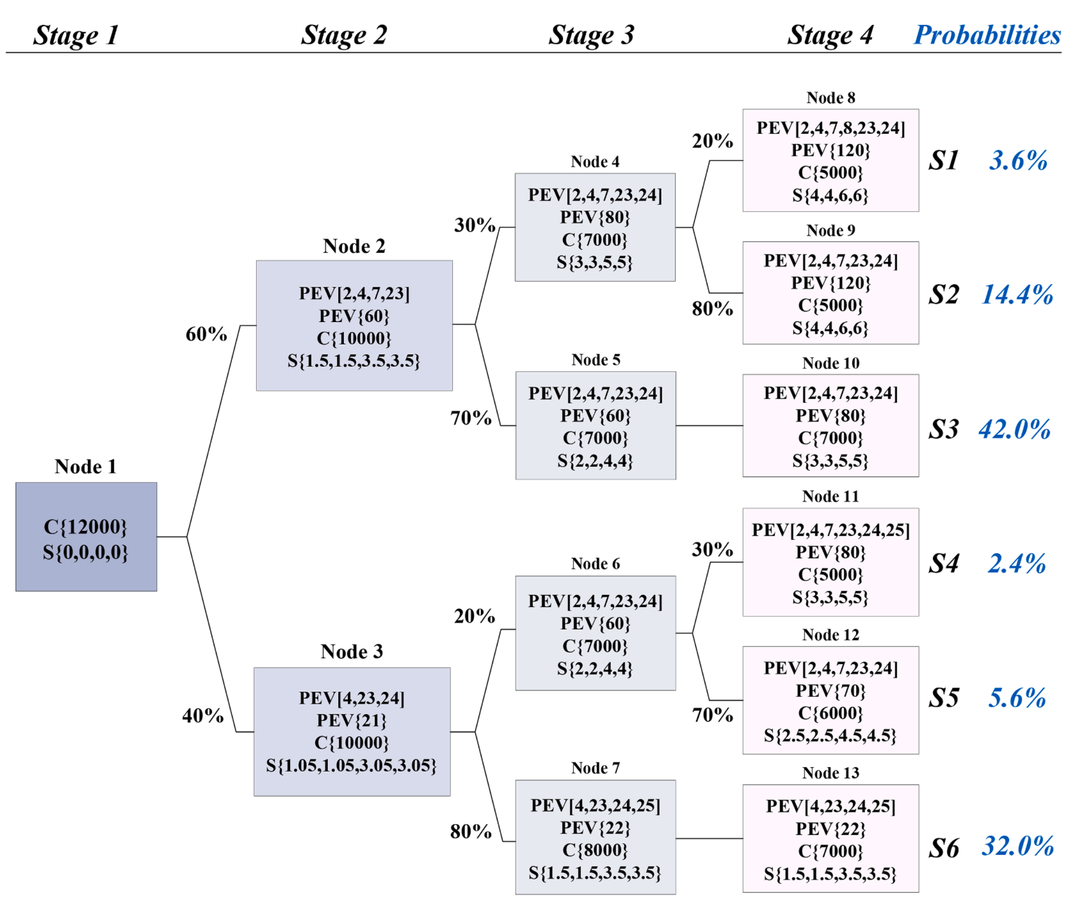

Fig. 3. Scenario tree illustrating uncertainties in the IEEE 33-bus distribution system.

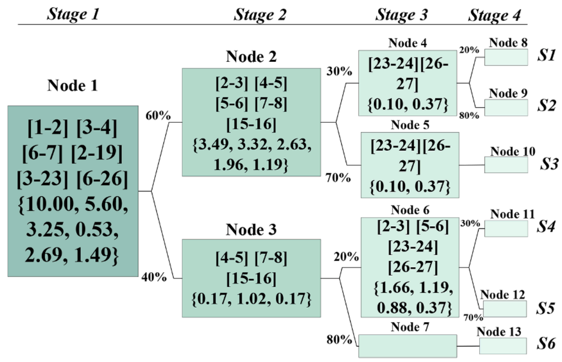

(a) FCS-only

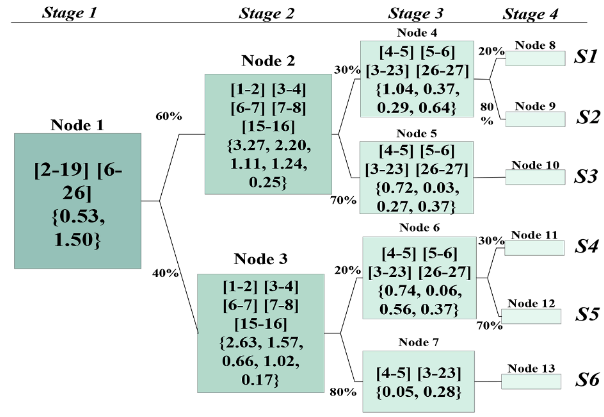

(b) ESS-FCS

Fig. 4. Optimal line investment strategies for IEEE 33-bus system: [.] is the invested line {.} is the upgraded capacity.

capacity. Fig. 5 maps these upgrades, using colour codes for planning stages (red: stage 1, orange: stage 2, blue: stage 3), and marks FC locations.

The uncertainties in Fig. 3 indicate that public EV demand strongly drives line upgrades. In Scenarios 1–3, upgrades begin with buses 1–8, creating transport hubs, then shift to the branch roads with buses 23–25. Scenarios 4–6 reverse this order, leading to different upgrade timings. For example, in Scenario 1, EV demand at bus 2 appears at stage 2, requiring FCS investment and an upgrade of line 2–3 to ensure an adequate power supply and avoid demand curtailment. In Scenario 4, however, public EV demand does not appear at bus 2 until node 6 (stage 3), delaying the upgrade of line 2–3. These variations demonstrate the value of multi-stage stochastic planning, which adapts investments to realized demand and avoids both premature upgrades (as would occur if planning followed Scenarios 1–3) and delayed responses that cause curtailments (as in Scenarios 4–6). This reflects how uncertainties in public EV development impact expansion planning and highlights the benefit of the proposed multi-stage stochastic planning framework in supporting strategic decision-making under uncertainty by allowing network investments to be delayed when appropriate (e.g., from node 2 in 2030 to node 4 in 2040). Such flexibility can generate cost savings by avoiding premature investments. For example, if a deterministic approach based on Scenarios 1–3 was adopted, upgrades would be implemented in 2030; however, if Scenarios 4 or 5 occurred instead, these investments would prove premature, resulting in unnecessary costs and inefficient asset utilization. In the worst case, under Scenario 6, the investments would become stranded. Conversely, if planning were based on Scenarios 4–6 but Scenarios 1–3 materialized, the delayed investment would lead to load curtailment from 2030 until upgrades were completed, incurring significant social and environmental costs. By contrast, the multi-stage stochastic model mitigates these risks and provides a more adaptive and resilient approach to expansion planning.

The ESS–FCS investment option further strengthens strategic decision-making under uncertainty. Conventional line upgrades involve complex licensing and lengthy construction [38], increasing the risk of delays and stranded assets under uncertainty. ESS-FCS helps mitigate this risk by providing flexibility in investment timing [39,40]. The differences between Fig. 4(a) and (b) demonstrate the ability of ESS-FCS to defer or displace conventional line reinforcements. Compared with the FCS-only case, upgrades of lines 1–2, 3–4, 6–7, and 3–23 which were originally upgraded in the root node, are relocated for upgrade; capacities of other lines are reduced; and line 2–3, initially scheduled at node 2, becomes unnecessary. In later stages, upgrades adjust dynamically to realized demand, with lines 1–2, 3–4, and 6–7 delayed to stage 2 at lower capacities, line 3–23 deferred to stage 3, and line 23–24 also displaced. This repositioning lowers line investment costs across all scenarios as shown in Fig. 6. Overall, ESS-FCS manages long-term uncertainty by deferring or reducing conventional reinforcements, thereby limiting overinvestment and reducing risk.

Expected costs shown in Table 3 indicate that ESS-FCS reduces traditional line investment by ~£0.09m, offsetting the additional cost of incorporating ESS, and yielding a net benefit of £0.01m in OV. Given the negligible impact of demand curtailment, FCS investment strategies are unaffected. The influence of the ESS-FCS on generation operations is also minimal due to the relatively minor installed PV capacity in the IEEE 33-bus system. ESS-FCS provides significant value by allowing

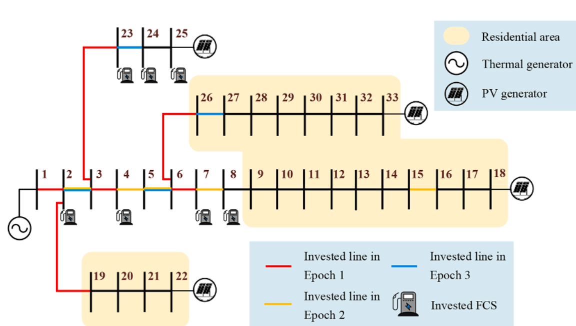

(a) FCS-only

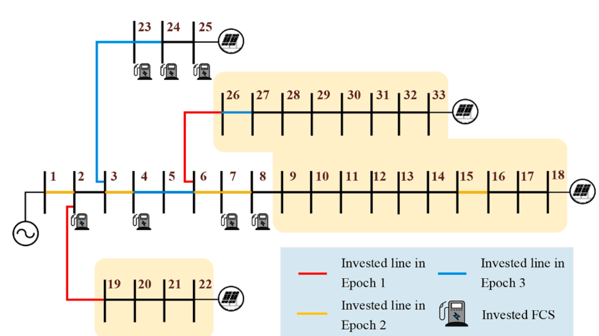

(b) ESS-FCS

Fig. 5. Maps of the optimal line investment strategies for IEEE 33-bus system with (a) FCS-only and (b) ESS-FCS.

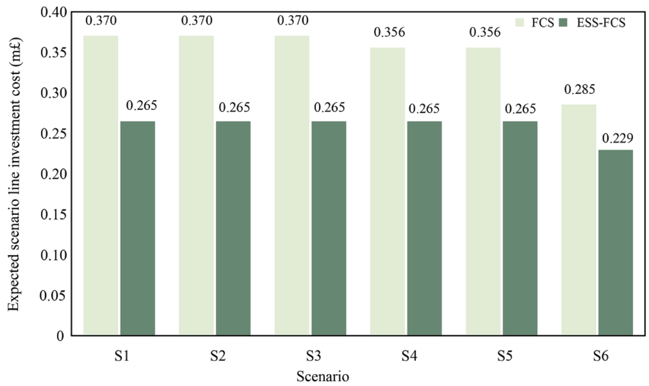

Fig. 6. The expected line investment costs per scenario for IEEE 33-bus system.

Table 3
Expected costs (in £ million) of IEEE 33-bus system.

	FCS	ESS-FCS
Total expected system cost	716.79	716.78
Total expected operational cost	715.94	715.94
Total expected investment cost	0.85	0.84
Line reinforcement	0.34	0.25
FCS	0.51	0.51
ESS	/	0.08
Option Value	/	0.01

postponement or avoidance of unnecessary investments, reducing premature expenditures and underutilization of network capacity. By enabling more flexible and adaptive planning, ESS-FCS helps mitigate the risk of stranded assets and ensures that investment decisions align closely with real-world conditions. Its long-term economic benefits are further examined in the Garver 6-bus transmission system in Section 4.2 and in sensitivity analysis regarding the impact of different PV capacity levels in Section 4.1.1.

4.1.1. *Sensitivity analysis of renewable generation capacities*

To examine how the OV of ESS-FCS changes with different levels of renewable penetration, this subsection extends the IEEE 33-bus distribution system by scaling the PV generation capacity to 2×, 4×, 6×, 8×, and 10× of the baseline in all scenario tree nodes. The results are illustrated in Fig. 7.

The results show a clear trend that as the share of renewable generation increases, the total expected system cost decreases because the system makes greater use of zero-marginal-cost PV generation. With more renewable energy available, ESS-FCS can store a larger share of surplus PV output and serve flexible charging demand more effectively. This leads to a reduction in the expected generation cost in the ESS-FCS case compared with the FCS-only case. Correspondingly, the OV of ESS-FCS increases from a very small value at the baseline PV capacity (£0.01m) to £0.96m (×4), £4.13m (×6), £6.14m (×8), and £10.21m (×10). This analysis highlights the growing environmental and economic value of ESS-FCS in systems with higher renewable penetration.

4.1.2. *Sensitivity analysis of scenario probabilities*

To validate the robustness of the planning approach, this section presents a sensitivity analysis testing alternative probability configurations that examines whether the investment outcomes and the OV of ESS-FCS remain stable when the likelihood of high- or low-growth futures changes. The probability settings of all cases are summarized in Table 4. Case A assigns higher probabilities to Scenario 1, which represents a high-stress future where network reinforcements are more urgent and the flexibility of ESS-FCS is expected to be particularly valuable. Case B places higher probability on the low-EV-growth Scenario 6, representing a conservative future with slower electrification and higher technology costs. Case C represents a highly uncertain future without a dominant trajectory with branching probabilities close to 0.5 at each stage.

The results are summarized in Table 5. Across all three configurations, the OV of ESS-FCS remains positive and even higher than in the baseline, which is consistent with the interpretation of ESS-FCS as a real option. Under Case A, the FCS-only strategy tends to over-invest early, exposing the system to stranded-asset risk when growth does not materialize in all scenarios. ESS-FCS mitigates this through deferrable and modular investments. For Case B, although it leads to lower expected demand pressure, it also creates a planning environment with

Table 4
The scenario probabilities of different cases.

	Baseline	Case A	Case B	Case C
S1	3.6 %	44.8 %	1.2 %	12.5 %
S2	14.4 %	11.2 %	4.8 %	12.5 %
S3	42.0 %	24.0 %	14.0 %	25.0 %
S4	2.4 %	11.2 %	4.8 %	12.5 %
S5	5.6 %	4.8 %	11.2 %	12.5 %
S6	32.0 %	4.0 %	64.0 %	25.0 %

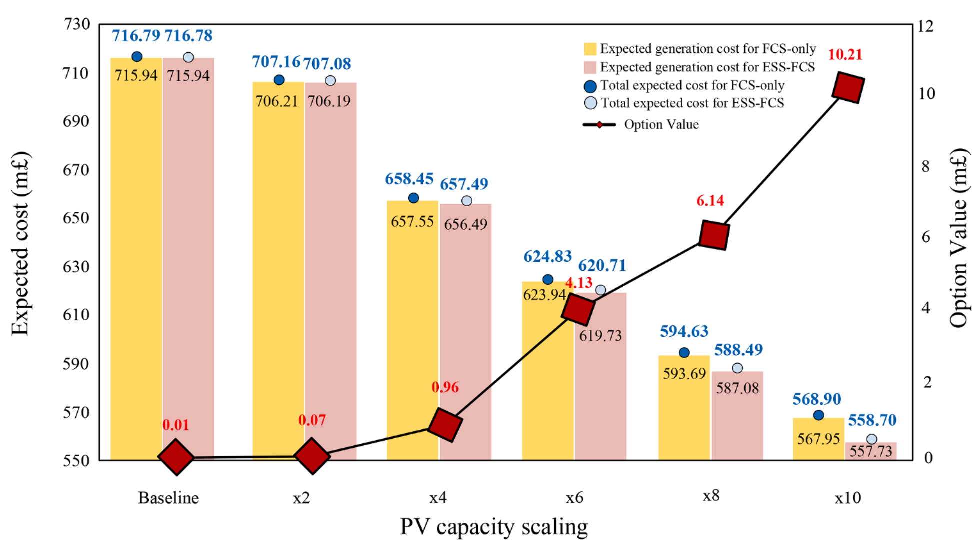

Fig. 7. Results under different PV capacity scaling.

Table 5
The expected results (in £ million) of different cases.

	Case A		Case B		Case C	
	FCS-only	FCS-ESS	FCS-only	FCS-ESS	FCS-only	ESS-FCS
total expected cost	722.12	703.50	701.04	700.85	717.09	717.06
Total expected operational cost	721.11	702.50	700.38	700.21	716.23	716.23
Total expected investment cost	1.01	1.00	0.66	0.64	0.85	0.83
Line reinforcement	0.36	0.26	0.30	0.24	0.34	0.26
FCS	0.65	0.65	0.36	0.36	0.51	0.51
ESS	/	0.08	/	0.04	/	0.06
OV	/	18.62	/	0.19	/	0.03

greater uncertainty and stronger cost asymmetry, which increases the relative value of flexible investment option of ESS-FCS. ESS-FCS provides a modular and deferrable alternative that can be built in smaller increments and adjusted as the actual demand unfolds. This flexibility reduces the risk of under-investment in an environment where demand and costs develop more slowly than expected. In the baseline and Case C, the FCS-only model adopts a moderate strategy under high uncertainty, resulting in lower but still positive OV.

Overall, this analysis demonstrates that the strategic and economic value of ESS-FCS is robust to a wide range of probability specifications. It provides a more rigorous justification for the scenario-tree probabilities and reinforces the credibility and robustness of the ESS-FCS OV identified in this study.

4.2. Economic value of ESS-FCS in transmission networks

A modified Garver 6-bus system [41] is used to evaluate the economic value of ESS-FCS in transmission networks. The modified system consists of 6 buses, 8 existing lines, and 3 generators with the following adjustments: 1) lines 2–6 and 4–6 exist but have limited capacity (10MW). 2) The thermal generator at bus 6 is replaced with a wind generator to introduce renewable generation and demonstrate the capability of ESS-FCS in managing such resources. 3) Public EVs account for 40 % of the total EVs.

Long-term uncertainty assumptions are summarized with Fig. 8. "EV [.]" indicates the multiplier of the number of EVs in a particular node, "C {.}" denotes FC unit investment cost (£/EV) and "W{.}" represents the installed wind capacity (MW) at bus 6. Fixed and variable line reinforcement costs are set as £70,000 /km and £70 /MW, respectively [36, 37,41], while other unit costs match those in the IEEE 33-bus system.

Table 6 summarizes expected costs for both models and the OV of ESS-FCS in the Garver 6-bus transmission system. "ESS" in the table refers to the storage component in ESS-FCS. The results show the investment and operational costs required to meet public EV charging demand under uncertainty, highlighting the economic advantage of ESS-FCSs with the OV indicating savings exceeding £130m. While the ESS-FCS incurs higher investment costs due to ESS integration, these are offset by reduced line reinforcement and generation operation costs. Specifically, line reinforcement costs drop by approximately £1.1m, a 21.8 % reduction, demonstrating enhanced network utilization and strategic investment flexibility.

Fig. 9 visualizes the optimal line investment strategies for both models, with red lines indicating transmission lines that require upgrades. With ESS-FCS, investment in line 3–5 is displaced, and upgrades to other lines are reduced, reflecting optimized timing and capacity decisions. This flexibility helps avoid unnecessary costs and enhances planning resilience. Moreover, operational cost reductions of approximately £138m underscore the efficiency of ESS-FCS utilizing renewable energy, highlighting its environmental benefit. Fig. 10 illustrates the expected generation costs across all scenarios; those for ESS-FCS are

Table 6
Expected costs (in £ million) of Garver 6-bus system.

	FCS	ESS-FCS
Total expected system cost	2401.68	2270.79
Total expected operational cost	2389.75	2251.56
Total expected investment cost	11.93	19.23
Line reinforcement	6.10	5.01
FCS	5.83	5.82
ESS	/	8.40
Option Value	/	130.89

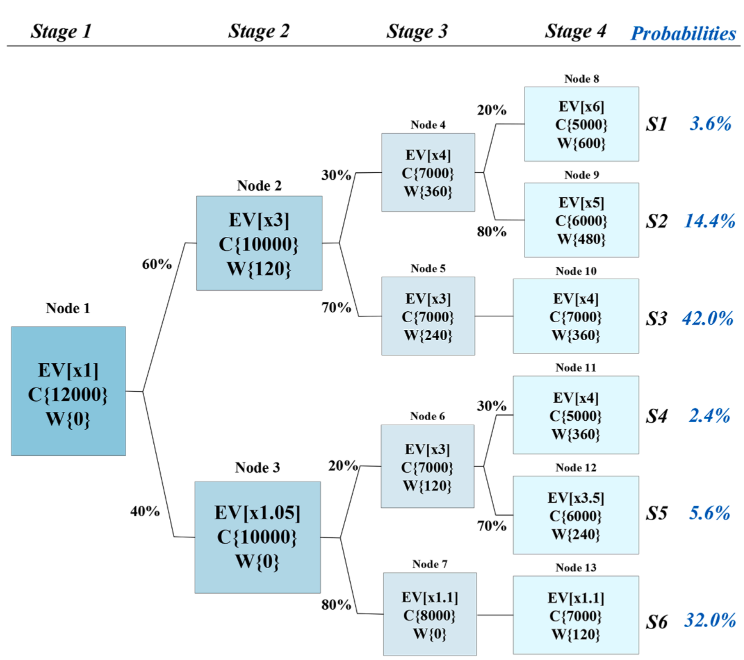

Fig. 8. Scenario tree illustrating uncertainties in the Garver 6-bus transmission system.

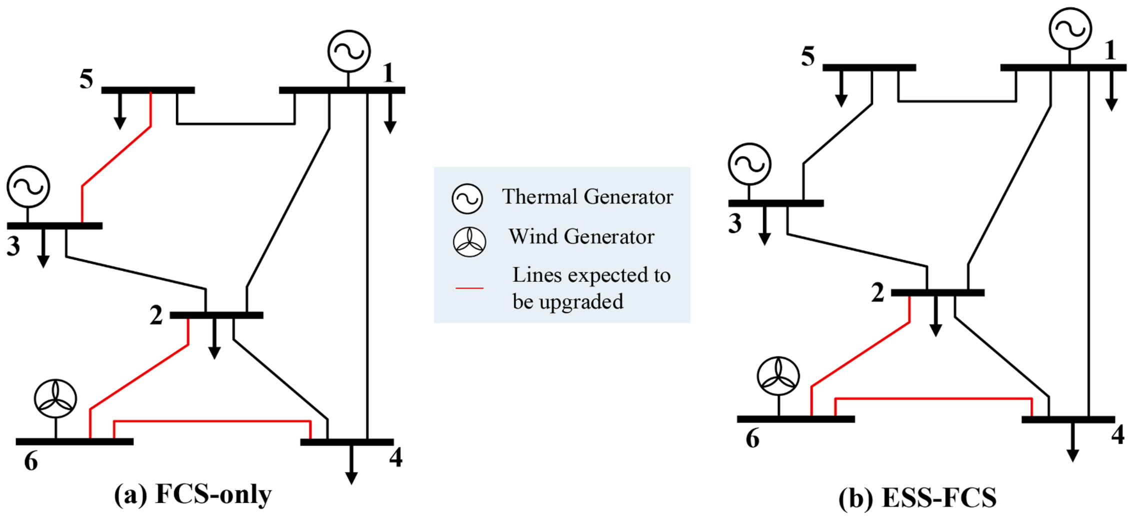

Fig. 9. Maps of the optimal line investment strategies for Garver 6-bus system with (a) FCS-only and (b) ESS-FCS.

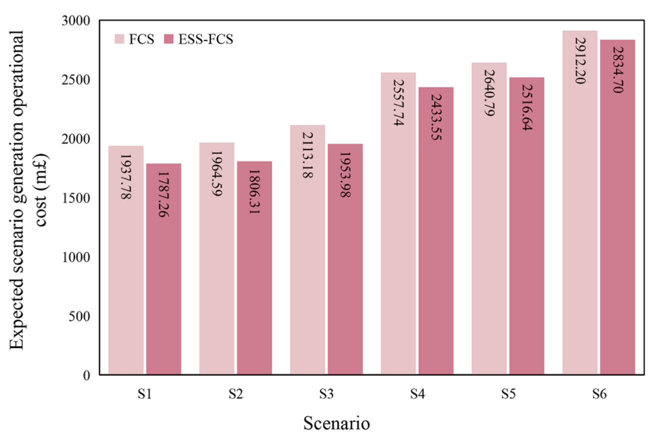

Fig. 10. The expected generation operational costs per scenario for Garver 6-bus system.

consistently lower reducing reliance on thermal generation and thereby mitigating CO_2 emissions. In contrast, the FCS-only model restricts renewable integration, increasing dependence on carbon-intensive thermal generators and consequently increasing system operation costs. Uncertainties surrounding the installed wind generation capacity significantly affect generator operations. As depicted in Fig. 8, wind capacity increases as the scenario progresses, while higher wind capacity correlates with reduced thermal reliance and lower generation costs. For example, although Scenarios 3 and 4 have identical final-stage wind capacity, Scenario 3 has higher installed capacity during stages 2 and 3. This difference explains the lower generation cost in Scenario 3 compared to that in Scenario 4.

Fig. 11 provides an overview of FCS investment strategies across all scenarios, which remain consistent between models due to minimal demand curtailment. Fig. 12 details expected FCS investment costs, influenced by fluctuations in FC unit costs and EV growth. It is evident that higher EV numbers lead to higher FCS investments, for instance, Scenario 1, characterized by the highest EV count, incurs the highest FCS investment cost of over £8.1m, while Scenario 6, with the lowest number of EVs, requires a significantly lower investment of under £3.3m, a notable difference of approximately £5m. A £1.8m gap between Scenarios 3 and 4 is attributed to FC unit cost differences, highlighting the impact of cost uncertainty on long-term planning.

4.2.1. Sensitivity analysis of fast charger ratings

This section presents a sensitivity analysis across three different FC ratings: 50 kW, 100 kW, and 150 kW. Fig. 13 shows that as FC rating increases, total expected costs also rise. However, ESS-FCS exhibits a more gradual increase and consistently lower costs than FCS-only.

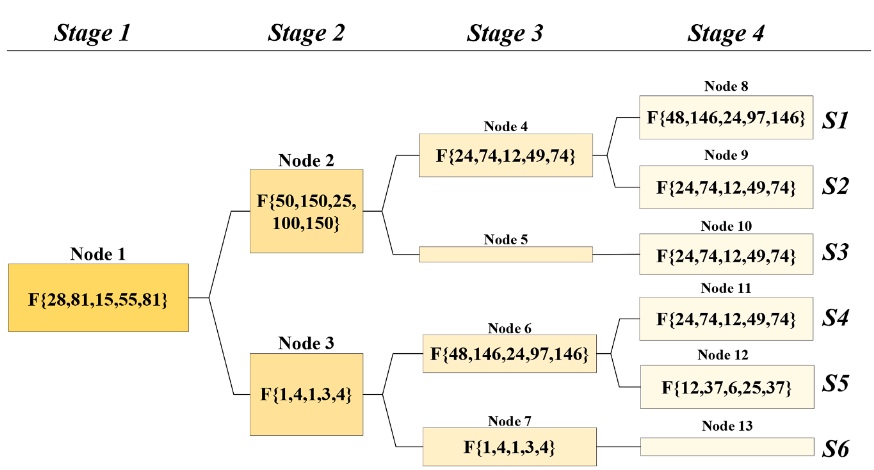

Fig. 11. Scenario tree of the optimal FCS investment strategies for Garver 6-bus system, where F{a,b,c,d,e} represents the number of FCs invested at bus 1,2,3,4, and 5.

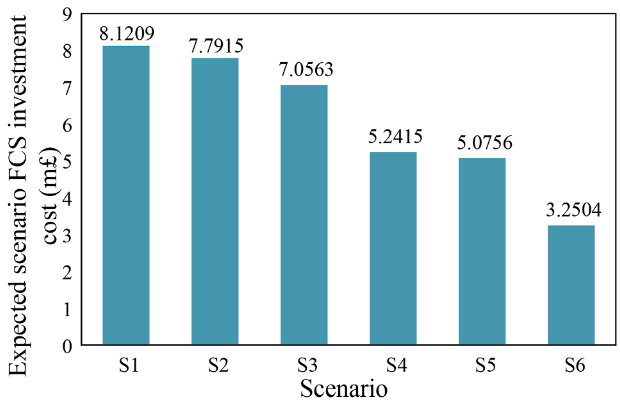

Fig. 12. The expected FCS investment costs per scenario for Garver 6-bus system.

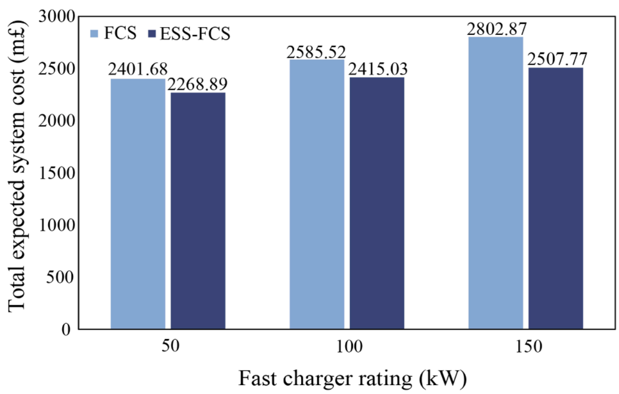

Fig. 13. The total expected system costs with different FC ratings and FCS models.

Table 7 details the OV for each rating, highlighting that ESS-FCS yields greater OV as FC rating increases. Fig. 14 illustrates that demand and generation costs rise with higher FC ratings for both models. Yet, ESS-FCS mitigates this cost escalation, achieving reductions of 5.86 %, 7.06 %, and 11.76 % compared to FCS-only as FC rating increases. This is due to ESS-FCS reducing thermal generation and emissions, enhancing environmental benefits.

Fig. 15 depicts expected line investment costs and capacity upgrades across the FC ratings and FCS models. Larger FC ratings favor ESS-FCS, offering enhanced economic benefits and flexibility in line upgrades. Compared to FCS-only, ESS-FCS reduces line investment costs by £1.09m (17.87 %) at 50 kW, £2.13m at 100 kW, and £2.30m (28.8 %) at 150 kW. Detailed changes in line investment are also illustrated, showing that while higher FC ratings require more capacity upgrades,

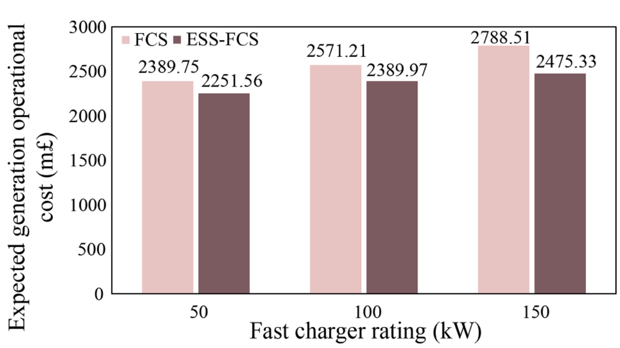

Fig. 14. The expected generation operational costs with different FC ratings and FCS models.

Table 7
OVs with different FC ratings.

	Option Value (£ million)
50 kW	130.89
100 kW	167.72
150 kW	292.06

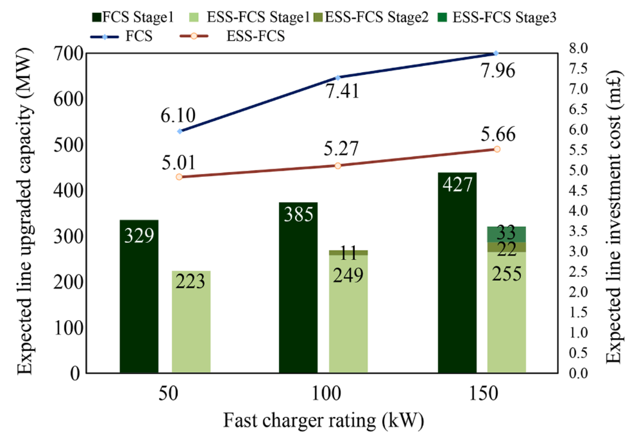

Fig. 15. The expected line upgraded capacities and line investment costs with different FC ratings and FCS models.

ESS-FCS alleviates congestion allowing to defer or displace upgrades to later stages.

4.3. Computational performance of the proposed framework

All numerical experiments were executed using FICO Xpress 8.10 on a personal computer equipped with an AMD Ryzen 5–4600H processor (6 cores / 12 threads, 3.00 GHz) and 16 GB RAM. By aggregating all test instances presented in the paper and computing the corresponding average total solution times, average number of Benders iterations, and the average time per iteration for each system, the results reported in Table 8 provide a representative indication of the computational burden. This averaging approach smooths out case-specific fluctuations and highlights the typical behavior of the algorithm across different scenarios.

A comparison of the average time per iteration shows that the increase observed in the ESS-FCS cases is primarily driven by the larger master problem and the additional investment variables. In the Garver 6-bus transmission system the average time per iteration remains relatively low, indicating that the subproblems are computationally light and scale efficiently. In contrast, the IEEE 33-bus distribution system exhibits higher per-iteration times, reflecting the heavier subproblem computations typical of larger distribution networks. Nevertheless, despite this increased per-iteration complexity, the ESS-FCS cases converge in fewer Benders iterations, resulting in a lower total solution time for the IEEE 33-bus system and demonstrating the advantage of the

Table 8
Computational performance.

		Solution time (s)	Iterations	Average time per iteration (s)
Garver 6-bus	FCS-only	190.69	33.00	5.78
	ESS-FCS	443.58	57.30	7.71
IEEE 33-bus	FCS-only	1531.48	56.57	27.07
	ESS-FCS	1320.67	44.43	29.73

Benders approach for more complex formulations.

Overall, the results show that the proposed solution method achieves reliable convergence across both systems. While total solution time naturally increases with network size and investment complexity, the per-iteration computational burden remains manageable, confirming the tractability of the method for multi-stage planning problems.

5. Conclusion

This paper presents a multi-stage stochastic network expansion planning framework to address long-term uncertainties in transmission and distribution systems, incorporating fast EV charging stations and energy storage systems. The framework supports strategic decision-making, allowing planners to adaptively delay, expand, or modify investments based on evolving system and market conditions. Two computationally efficient FCS models are proposed, one standalone and one with integrated ESS, for incorporation into large-scale planning. The ESS-FCS model demonstrates significant strategic and economic advantages over the FCS-only approach. Quantitative results from case studies show that ESS-FCS reduces expected line reinforcement costs by up to 28.8 % and achieves operational cost savings exceeding £138 million in transmission networks, showcasing that the ESS-FCS model enhances planning flexibility by helping mitigate risks of stranded assets, premature expenditures, and network underutilization, thereby improving long-term economic outcomes.

Real Option valuation highlights the flexibility benefits of ESS-FCS, with option values ranging from £0.01 million in distribution systems to £130.89 million in transmission systems, and up to £292.06 million under high charger ratings. The scale of these benefits naturally depends on system characteristics such as renewable penetration, network topology, charging demand patterns, and underlying uncertainties. Across all cases, ESS-FCS consistently mitigates stranded-asset risks, defers costly reinforcements, and supports higher renewable utilization, delivering strong economic performance under uncertainty. These results underscore the substantial potential of ESS-FCS while highlighting the importance of system-specific assessment when evaluating its economic impact. Together, the findings demonstrate how flexible charging infrastructure can enhance long-term planning outcomes and contribute to cost-effective pathways toward net-zero power systems. Future research could extend the framework by incorporating age-dependent operation cost models for assets, enabling more detailed lifecycle representations where such data are available, and by investigating practical risk implications of different expansion planning formulations to reflect the needs of system planners in understanding a wider range of strategic developments.

CRediT authorship contribution statement

Yuxin Sun: Writing – original draft, Visualization, Software, Methodology, Investigation, Formal analysis. **Stefan Borozan:** Writing – review & editing, Validation, Methodology, Data curation, Conceptualization. **Tala El Samad:** Writing – review & editing, Supervision, Formal analysis. **Guibin Wang:** Writing – review & editing, Supervision. **Goran Strbac:** Supervision, Resources, Project administration.

Declaration of competing interest

The authors declare that they have no known competing financial interests or personal relationships that could have appeared to influence the work reported in this paper.

Data availability

All data supporting the findings of this study are included in the article references.

References

[1] X. Sun, H. Xie, D. Qiu, Y. Xiao, G. Strbac, Z. Bie, Incentivizing EVs to provide frequency regulation services by aggregative game-based mechanism, IEEE Trans. Veh. Technol. 73 (9) (2024) 12787–12800, https://doi.org/10.1109/TVT.2024.3396212.

[2] UNFCCC, The Paris Agreement, 2015,Available: https://unfccc.int/process-and-meetings/the-paris-agreement?gad_source=1&gclid=CjwKCAjwnei0BhB-EiwAA2xuBi6hI4GS3mhT8YfiKRvVwFzvuQUlZP4Gg0roKAKOfJNljl0AzMsu7xoCMIAQAvD_BwE.

[3] HM Government, Net Zero Strategy: Build Back Greener, UK Government, 2021, Available: https://assets.publishing.service.gov.uk/government/uploads/system/uploads/attachment_data/file/1033990/net-zero-strategy-beis.pdf.

[4] S. Giannelos, et al., Long-term expansion planning of the transmission network in India under multi-dimensional uncertainty, Energies 14 (22) (2021) 7813, https://doi.org/10.3390/en14227813.

[5] T. Wu, X. Wei, X. Zhang, G. Wang, J. Qiu, S. Xia, Carbon-oriented expansion planning of integrated electricity-natural gas systems with EV fast-charging stations, IEEE Trans. Transp. Electrification 8 (2) (2022) 2797–2809, https://doi.org/10.1109/TTE.2022.3151811.

[6] M.C. Falvo, M. Manganelli, C. Moscatiello, F. Vellucci, Electrical vehicles and charging stations: state of art and future perspectives, in: 2022 IEEE International Conference on Environment and Electrical Engineering and 2022 IEEE Industrial and Commercial Power Systems Europe (EEEIC /I&CPS Europe), 2022, pp. 1–7, https://doi.org/10.1109/EEEIC/ICPSEurope54979.2022.9854740.

[7] A. Hussain, V.-H. Bui, H.-M. Kim, Optimal sizing of battery energy storage system in a fast EV charging station considering power outages, IEEE Trans. Transp. Electrification 6 (2) (2020) 453–463, https://doi.org/10.1109/TTE.2020.2980744.

[8] Y. Tao, J. Qiu, S. Lai, X. Sun, J. Zhao, Adaptive integrated planning of electricity networks and fast charging stations under electric vehicle diffusion, IEEE Trans. Power Syst. 38 (1) (2023) 499–513, https://doi.org/10.1109/TPWRS.2022.3167666.

[9] G. Zhou, Q. Dong, Y. Zhao, H. Wang, L. Jian, Y. Jia, Bilevel optimization approach to fast charging station planning in electrified transportation networks, Appl. Energy 350 (2023) 121718, https://doi.org/10.1016/j.apenergy.2023.121718.

[10] M. Asna, H. Shareef, P. Achikkulath, H. Mokhlis, R. Errouissi, A. Wahyudie, Analysis of an optimal planning model for electric vehicle fast-charging stations in Al Ain City, United Arab Emirates, IEEE Access 9 (2021) 73678–73694, https://doi.org/10.1109/ACCESS.2021.3081020.

[11] J. Feng, Z. Hu, X. Duan, EV fast charging station planning considering competition based on stochastic dynamic equilibrium, IEEE Trans. Ind. Appl. 59 (3) (2023) 3795–3809, https://doi.org/10.1109/TIA.2023.3235343.

[12] D. Sbordone, I. Bertini, B. Di Pietra, M.C. Falvo, A. Genovese, L. Martirano, EV fast charging stations and energy storage technologies: a real implementation in the smart micro grid paradigm, Electr. Power Syst. Res. 120 (2015) 96–108, https://doi.org/10.1016/j.epsr.2014.07.033.

[13] B. Sun, A multi-objective optimization model for fast electric vehicle charging stations with wind, PV power and energy storage, J. Clean. Prod. 288 (2021) 125564, https://doi.org/10.1016/j.jclepro.2020.125564.

[14] H. Ding, Z. Hu, Y. Song, Value of the energy storage system in an electric bus fast charging station, Appl. Energy 157 (2015) 630–639, https://doi.org/10.1016/j.apenergy.2015.01.058.

[15] J. Wang, Q. Guo, H. Sun, Planning approach for integrating charging stations and renewable energy sources in low-carbon logistics delivery, Appl. Energy 372 (2024) 123792, https://doi.org/10.1016/j.apenergy.2024.123792.

[16] T.S. Bryden, G. Hilton, B. Dimitrov, C. Ponce de León, A. Cruden, Rating a stationary energy storage system within a fast electric vehicle charging station considering user waiting times, IEEE Trans. Transp. Electrification 5 (4) (2019) 879–889, https://doi.org/10.1109/TTE.2019.2910401.

[17] H. Mehrjerdi, R. Hemmati, Stochastic model for electric vehicle charging station integrated with wind energy, Sustain. Energy Technol. Assess. 37 (2020) 100577, https://doi.org/10.1016/j.seta.2019.100577.

[18] M. Gjelaj, C. Træholt, S. Hashemi, P.B. Andersen, Cost-benefit analysis of a novel DC fast-charging station with a local battery storage for EVs, in: 2017 52nd International Universities Power Engineering Conference (UPEC), 2017, pp. 1–6, https://doi.org/10.1109/UPEC.2017.8231973.

[19] A. Carruth, A. Dickerson, A. Henley, What do we know about investment under uncertainty? J. Econ. Surv. 14 (2) (2000) 119–154, https://doi.org/10.1111/1467-6419.00107.

[20] A.K. Dixit, R.S. Pindyck, Investment Under Uncertainty, Princeton University Press, 1994, https://doi.org/10.2307/j.ctt7sncv.

[21] J. Jurčević, I. Pavić, N. Čović, D. Dolinar, D. Zoričić, Estimation of internal rate of return for battery storage systems with parallel revenue streams: cycle-cost vs. Multi-objective optimisation approach, Energies 15 (16) (2022) 16, https://doi.org/10.3390/en15165859. Art. no.

[22] J.A. Schachter, P. Mancarella, A critical review of Real Options thinking for valuing investment flexibility in Smart Grids and low carbon energy systems, Renew. Sustain. Energy Rev. 56 (2016) 261–271, https://doi.org/10.1016/j.rser.2015.11.071.

[23] M. Kozlova, Real option valuation in renewable energy literature: research focus, trends and design, Renew. Sustain. Energy Rev. 80 (2017) 180–196, https://doi.org/10.1016/j.rser.2017.05.166.

[24] I. Konstantelos, S. Giannelos, G. Strbac, Strategic valuation of smart grid technology options in distribution networks, IEEE Trans. Power Syst. 32 (2) (2017) 1293–1303, https://doi.org/10.1109/TPWRS.2016.2587999.

[25] S. Borozan, S. Giannelos, G. Strbac, Strategic network expansion planning with electric vehicle smart charging concepts as investment options, Adv. Appl. Energy 5 (2022) 100077, https://doi.org/10.1016/j.adapen.2021.100077.
[26] S. Borozan, S. Giannelos, M. Aunedi, G. Strbac, Option value of EV smart charging concepts in transmission expansion planning under uncertainty, in: 2022 IEEE 21st Mediterranean Electrotechnical Conference (MELECON), IEEE, Palermo, Italy, 2022, pp. 63–68, https://doi.org/10.1109/MELECON53508.2022.9842982.
[27] F. Penizzotto, R. Pringles, F. Olsina, Real options valuation of photovoltaic power investments in existing buildings, Renew. Sustain. Energy Rev. 114 (2019) 109308, https://doi.org/10.1016/j.rser.2019.109308.
[28] I. Konstantelos, G. Strbac, Valuation of flexible transmission investment options under uncertainty, IEEE Trans. Power Syst. 30 (2) (2015) 1047–1055, https://doi.org/10.1109/TPWRS.2014.2363364.
[29] Y. Xiao, W. Wu, X. Wang, Y. Qu, J. Li, Economic potentials of energy storage technologies in electricity markets with renewables, Energy Storage Sav. 2 (1) (2023) 370–391, https://doi.org/10.1016/j.enss.2022.10.004.
[30] D. de S. Santos, T.A.E. Ferreira, Neural network learning of black-scholes equation for option pricing, *arXiv*: arXiv:2405.05780. Accessed: Jul. 19, 2024. [Online]. Available, http://arxiv.org/abs/2405.05780, May 09, 2024.
[31] J. Balibrea-Iniesta, Economic analysis of renewable energy regulation in France: a case study for photovoltaic plants based on real options, Energies 13 (11) (2020) 11, https://doi.org/10.3390/en13112760. Art. no.
[32] S.H. Dolatabadi, M. Ghorbanian, P. Siano, N.D. Hatziargyriou, An enhanced IEEE 33 bus benchmark test system for Distribution System studies, IEEE Trans. Power Syst. 36 (3) (2021) 2565–2572, https://doi.org/10.1109/TPWRS.2020.3038030.
[33] UK Department for Transport, National Travel Survey: 2022, GOV.UK, 2022,'National Travel Survey: 2022′, GOV.UK. Available: https://www.gov.uk/government/statistics/national-travel-survey-2022.
[34] UK Department for Business, Energy & Industrial Strategy (BEIS), Electricity Storage Costs: Technical Assumptions, 2018, Available: https://assets.publishing.service.gov.uk/government/uploads/system/uploads/attachment_data/file/910261/storage-costs-technical-assumptions-2018.pdf.
[35] International Council on Clean Transportation (ICCT), Estimating Electric Vehicle Charging Infrastructure Costs across Major U.S. Metropolitan Areas, 2019, Available: https://theicct.org/publication/estimating-electric-vehicle-charging-infrastructure-costs-across-major-u-s-metropolitan-areas/.
[36] Greater London Authority (GLA), Low Carbon London Electric Vehicle Load Profiles, London Datastore, 2015, Available: https://data.london.gov.uk/dataset/low-carbon-london-electric-vehicle-load-profiles.
[37] Agency for the Cooperation of Energy Regulators (ACER), Unit Investment Cost Indicators - Project Support to ACER, 2023, Available: https://www.acer.europa.eu/sites/default/files/documents/Publications/UIC_report_2023.pdf.
[38] Energy Systems Catapult, Electricity Networks Commissioner: Companion Report – Findings and Recommendations, 2023, Available: https://assets.publishing.service.gov.uk/media/64c8e85219f5622360f3c0ee/electricity-networks-commissioner-companion-report.pdf.
[39] SP Energy Networks, PACE Closeout Report, 2020, Available: https://www.spenergynetworks.co.uk/userfiles/file/PACE_Closeour_Report.pdf.
[40] Transport Scotland, Delivering the Vision – Installing Refuelling and Charging Infrastructure, 2022, Available: https://www.transport.gov.scot/publication/final-report-on-the-work-of-the-zero-emission-mobility-industry-advisory-group/delivering-the-vision-installing-refuelling-and-charging-infrastructure/.
[41] L.L. Garver, Transmission network estimation using linear programming, IEEE Trans. Power Appar. Syst. PAS-89 (7) (1970) 1688–1697, https://doi.org/10.1109/TPAS.1970.292825.